Korean J. Chem. Eng., **24**(2), 319-327 (2007)

Aggregation mechanism of fine fly ash particles in uniform magnetic field

Yong-Wang Li, Chang-Sui Zhao†, Xin Wu, Duan-Feng Lu and Song Han

Key Laboratory of Clean Coal Power Generation and Combustion Technology of Ministry of Education, Southeast University, Nanjing 210096, China
(*Received 25 August 2006 • accepted 21 October 2006*)

Abstract−Aggregation of fly ash particles with size range of 0.023-9.314 μm in a uniform magnetic field was investigated for removing them. A binary collision-aggregation model evaluating particle aggregation coefficient was developed. Based on the model, particle removal efficiency was calculated by solving the General Dynamic Equation. The comparison was done between the calculated and experimental data. The modeling aggregation coefficient shows that the aggregation coefficient increases with particle size, and the bigger the size difference between two particles is, the more strongly the gravity difference promotes aggregation. For the mid-sized particles, their removal efficiencies are higher than those of the smaller and bigger ones. The effect of the magnetic flux density on total particle removal efficiency is similar to that on aggregation coefficient. Before particles are saturatedly magnetized, their total removal efficiency increases with an increase in the magnetic flux density. Higher removal efficiency can also be caused by prolonging the particle residence time in the magnetic field or increasing their mass concentration. The particle number median diameter decreases with an increase in the total removal efficiency. Calculation results are found to coincide essentially with the experimental data.

Key words: Fly Ash Particles, Aggregation, Aggregation Coefficient, Removal Efficiency, Magnetic Field

INTRODUCTION

PM_{10} has been of increasing concern for its association with increased mortality, morbidity and decreased lung function [1,2], especially emitted from coal combustion sources in China [3]. Because of tiny volume, less weight and enormous number of the fine fly ash particles from coal combustion, the conventional dust removal facilities have little effect on them. There are two ways to remove them from flue gas. One is to remove them directly by new-style facilities; the other is to enlarge them by aggregation first, and then to remove the bigger ones by conventional dust facilities. Particle aggregation results from inter-particle collisions, which are induced by their relative motion. The fly ash particle body is composed of aluminosilicate, blended with or infiltrated into its crystal lattice by ferric oxide and other metal oxides [4,5], so that it can be magnetized easily in a magnetic field [6]. Under the action of primary forces, including drag, Brownian, and gravity, as well as van der Waals and magnetic dipole inter-particle forces, the fine fly ash particles collide with one another and stick together during passing through an external magnetic field. Thus, a promising way of removing the fine fly ash particles from flue gas is to aggregate the fine fly ash particles by an external magnetic field, and the project of investigation on that was launched as one of the National Basic Research Programs of China.

The study on particle collision and aggregation has wide interest because of its applicability to many practical systems. Magnetic separation has been suggested as a recovery and pollution control process, such as for the separation and concentration of mining ores and waste [7], for desulphurization of coal [8] and for effluent from steel mills [9]. Zarutskaya and Shapiro [10] developed a physical-mathematical model describing the motion and collection of orientable nanoparticles from airflow in magnetic filters. A strong dependence of the capture efficiency on the particle diameter was found for the particle with size less than 0.2 μm. Aggregation of small dust grains also results in interesting structures of the aggregates such as single chains and inter-connected web-like structures [11]. The aggregation process could be used to enhance the removal efficiency of high-gradient magnetic separations [12,13]. Particle aggregation in a magnetic field has also been used for delivering therapeutic drugs [14] and purifying drinking water [15].

There have been some investigations on the collision and aggregation of particles in a magnetic field. Based on the Brownian coagulation model, Svoboda [16] considered the flocculation of weakly magnetic quasi-colloidal particles in suspensions, using an inter-particle force potential that includes electrical double layer, van der Walls and magnetic forces. Aggregation of small dust grains is considered the basic mechanism forming planetesimals and cometesimals in the solar system, and the properties of dust aggregation driven by magnetic dipole force were discussed by Dominik and Nübold [17]. By making mathematical approximations, Prakash and Pratim [18] derived the expression of collision frequency function for particles whose dipoles are randomly oriented and aligned in magnetic fields, neglecting all but the magnetic dipole force potential.

Though several experimental and theoretical studies have been carried out to study the aggregation of magnetic particles, most of the study objects are coarse particles in liquid. No reliable theoretical model exists that would predict the behavior of fine fly ash particles in an external magnetic field. To better understand the aggregation mechanism of fine fly ash particles from coal combustion,

†To whom correspondence should be addressed.
E-mail: cszhao@seu.edu.cn
‡This paper was presented at the 6th Korea-China Workshop on Clean Energy Technology held at Busan, Korea, July 4-7, 2006

and provide a solid basis for the application in practice of particle aggregation in an external magnetic field, in this paper, a binary collision-aggregation model was developed for evaluating the aggregation coefficient of fine particles in a uniform magnetic field. The acquired aggregation coefficient and the particle size distribution then were used to predict the removal efficiencies and number median diameter of fine fly ash particles from boiler firing bituminous coal, and the prediction results were compared with the experimental data.

KINETICS OF PARTICLE AGGREGATION

Binary collision-aggregation is the dominant mode of particle aggregation which results in the variation of particle number concentration [19]. The variation rate can be predicted by the General Dynamic Equation (GDE) [20]:

$$\frac{\partial n(v,t)}{\partial t}=\underbrace{\frac{1}{2}\int_{v_{min}}^{v}\beta(u,v-u)n(u,t)n(v-u,t)du}_{\text{aggregation gain}}-\underbrace{n(v,t)\int_{v_{min}}^{v_{max}}\beta(u,v)n(u,t)du}_{\text{aggregation loss}} \quad (1)$$

Where, $\beta(u, v)$ is the aggregation coefficient between two particles whose volumes are u and v, n(v, t) is the size distribution function, n(v, t)dv is the number concentration of particles in the volume range [v, v+dv] at time t, v_{min} is the minimum volume of particles existing in gas flow at time t, and v_{max} is the maximum one. The first term on the right-hand side of Eq. (1) represents the conversion rate of particles with volume u and volume v−u into volume v. The second term represents the conversion rate of particles with volume v to bigger particles through collisions with the rest of the distribution. On condition that particle size distribution and aggregation coefficient are known, the variation rate of particle number concentration can be determined through solving the GDE with numerical method. The particle size distribution can be measured by the particle measurement apparatus, and the aggregation coefficient can be evaluated by the binary collision-aggregation model.

BINARY COLLISION-AGGREGATION MODEL

It is well-known that the Brownian aggregation coefficient β_B between two particles is given by [21]

$$\beta_B=2\pi(d_i+d_j)(D_i+D_j) \quad (2)$$

Where, D_i and D_j are the diffusion coefficients of particles i and j, and d_i and d_j are their diameters. For magnetized particles, their coefficient β_{mag} is modified as follows [18]:

$$\beta_{mag}=\frac{\beta_B}{\left(\frac{d_i+d_j}{2}\right)\int_{(d_i+d_j)/2}^{\infty}\frac{1}{r^2}\exp\left(\frac{\psi}{kT}\right)dr} \quad (3)$$

Where, r is the center-to-center distance of the two particles, k is the Boltzmann constant, T is the absolute temperature, and ψ is the magnetic potential between two particles.

The aggregation coefficient derived from Eq. (2) and (3) is based on particle Brownian motion. Thus, Eq. (3) cannot be applied when particle motion is mainly influenced by various forces, including drag, Brownian and gravity, as well as magnetic dipole, and van der Waals inter-particle forces. Therefore, a new model is urgently needed for aggregation coefficient of magnetized particles in the external magnetic field.

The aggregation coefficient is an effective collision volume between two interacting particles per unit time [22]. According to its physical meaning, it can be calculated by tracing the trajectories of two interacting particles.

1. Particle Motion Equations

The fine fly ash particles transported into uniform magnetic field by gas flow are subjected to various forces, including magnetic dipole, drag, Brownian, van der Waals and gravity, and their three-dimensional motion equations in rectangular cartesian coordinate system can be expressed as

$$\begin{cases}\frac{\pi\rho_p d_p^3}{6}\frac{d^2x}{dt^2}=F_{mag,x}+F_{d,x}+F_{B,x}+F_{V,x}\\ \frac{\pi\rho_p d_p^3}{6}\frac{d^2y}{dt^2}=F_{mag,y}+F_{d,y}+F_{B,y}+F_{V,y}+F_g\\ \frac{\pi\rho_p d_p^3}{6}\frac{d^2z}{dt^2}=F_{mag,z}+F_{d,z}+F_{B,z}+F_{V,z}\end{cases} \quad (4)$$

Where, ρ_p is the particle density, d_p is the particle diameter, F is the forces exerting on the particle, the subscripts mag, d, B, W, g represent the action forces of magnetic dipole, drag, Brownian, Van der Waals and gravity, and the subscripts x, y, z are the forces components along the x-axis, y-axis and z-axis, respectively.

1-1. Magnetic Dipole Force

In a uniform magnetic field, the fly ash particles are magnetized and become magnetic dipoles. The magnetic moment vectors of particles i and j are $\mathbf{m}_{o,i}$ and $\mathbf{m}_{o,j}$, as shown in Fig. 1. The interacting force $\mathbf{F}_{mag}$ between two magnetic dipoles is given by

$$\mathbf{F}_{mag}=\nabla(\mu_0\mathbf{m}_{o,j}\cdot\nabla\varphi_i) \quad (5a)$$

$$\varphi_i=\frac{1}{4\pi}\left(\frac{\mathbf{m}_{o,i}\cdot\mathbf{r}}{r^3}\right) \quad (5b)$$

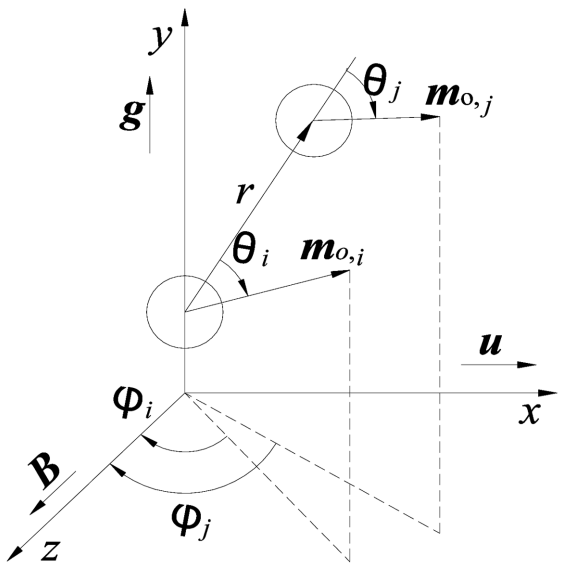

Fig. 1. Geometrical representation of interacting particles.

Where, μ_0 is the permeability of free space, and φ_i is the magnetic scalar potential of particle i.

Thus the radial and tangential components of magnetic dipole force can be derived from Eq. (5a) and Eq. (5b) as follows:

$$F_{mag,r}=\frac{3\mu_0 m_{o,i}m_{o,j}[3\cos(\theta_i)\cos(\theta_j)-\cos(\phi_j-\phi_i)]}{4\pi r^4} \quad (6a)$$

$$F_{mag,\theta}=-\frac{3\mu_0 m_{o,i}m_{o,j}\sin(\theta_i+\theta_j)}{4\pi r^4} \quad (6b)$$

Where, θ_i is the angle between $\mathbf{m}_{o,i}$ and radial direction r, θ_j is the angle between $\mathbf{m}_{o,j}$ and radial direction r, and $|\Phi_j-\Phi_i|$ is the angle between the two magnetic moment vectors. For the magnetic dipoles, their moment vectors are all aligned in the direction of the external magnetic field so that θ_i is equal to θ_j and Φ_i is equal to Φ_j. Therefore, the magnetic dipole force can be written by

$$F_{mag,r}=\frac{3\mu_0 m_{o,i}m_{o,j}[3\cos^2(\theta)-1]}{4\pi r^4} \quad (7a)$$

$$F_{mag,\theta}=-\frac{3\mu_0 m_{o,i}m_{o,j}\sin(2\theta)}{4\pi r^4} \quad (7b)$$

Magnetic moment vector $\mathbf{m}_o$ can be expressed in magnetization vector **M**, given by

$$\mathbf{m}_o=\frac{\pi d_p^3}{6}\mathbf{M} \quad (8)$$

Substituting Eq. (8) for the value $\mathbf{m}_o$ in Eq. (7a) and Eq. (7b), we get

$$F_{mag,r}=\frac{\pi\mu_0 M^2 d_i^3 d_j^3[3\cos^2(\theta)-1]}{48r^4} \quad (9a)$$

$$F_{mag,\theta}=-\frac{\pi\mu_0 M^2 d_i^3 d_j^3\sin(2\theta)}{48r^4} \quad (9b)$$

Fig. 2 is an illustration of direction and relative magnitude of magnetic dipole force for two aligned magnetic dipoles, and it identifies the regions where the interaction would be attractive and repulsive. Depending on the polar angle θ, the interaction between dipoles would be attractive ($3\cos^2(\theta)-1>0$) or repulsive ($3\cos^2(\theta)-1<0$). Furthermore, the force lines between the two magnetic dipoles (Fig. 3) indicate that the magnetic dipole located in the repulsive region would enter the attractive region under the radial and tangential force of magnetic dipoles, and finally they come into close proximity and adhere together.

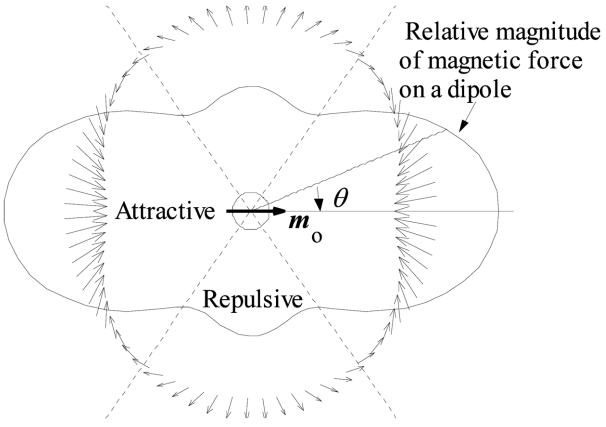

Fig. 2. Direction and relative magnitude of magnetic dipole force.

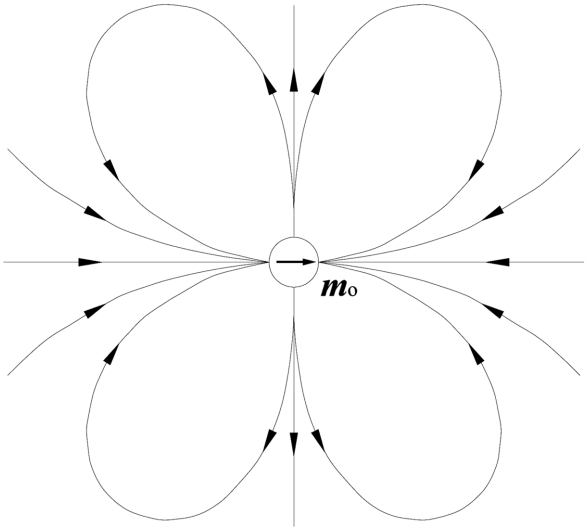

Fig. 3. Force lines between two magnetic dipoles.

1-2. Drag Force

In the Stocks flow regime, the drag force, $\mathbf{F}_d$, over a free-moving particle is given by [23]

$$\mathbf{F}_d=\frac{3\pi\mu d_p}{C_c}(\mathbf{u}_f-\mathbf{v}_p) \quad (10a)$$

$$C_c=1+\frac{2.514+0.80\exp(-0.55d_p/\lambda)}{d_p/\lambda} \quad (10b)$$

Where, μ is dynamic viscosity, $\mathbf{u}_f$ is the gas flow velocity, $\mathbf{v}_p$ is the particle velocity, and C_c is the Cunningham correction factor when the particle size is in the molecular region, λ is mean free path of gas molecules.

1-3. Brownian Force

The Brownian force F_B is modeled by using a Gaussian random number with zero-mean unit-variation, G, as [24]

$$F_B=G\sqrt{\frac{6\pi d_p\mu kT}{\Delta t}} \quad (11)$$

Where, Δt is the magnitude of time step.

1-4. Van der Waals Force

The van der Waals interaction between two particles separated by a distance h (surface-to-surface) is given by [25]

$$\mathbf{F}_w=-\frac{A(16\chi)^3}{3(d_i+d_j)}\left[\frac{2s}{(1+\chi)^2(s^2-4)^2[s^2(1+\chi)^2-4(1-\chi)^2]^2}\right]\mathbf{e}_r \quad (12a)$$

Where, A is the Hamaker constant, $\mathbf{e}_r$ is the unit vector in the radial direction, and

$$s=\frac{2(2h+d_i+d_j)}{d_i+d_j} \quad (12b)$$

$$\chi=\frac{d_i}{d_j} \quad (12c)$$

Fig. 4 shows the dimensionless of van der Waals force to magnetic dipole radial force (θ=0) as functions of the surface-to-surface separation between two magnetized particles at $A=0.4\times10^{-20}$ J and $M=2.5\times10^3$ A m^{-1}. The dimensionless force decreases significantly

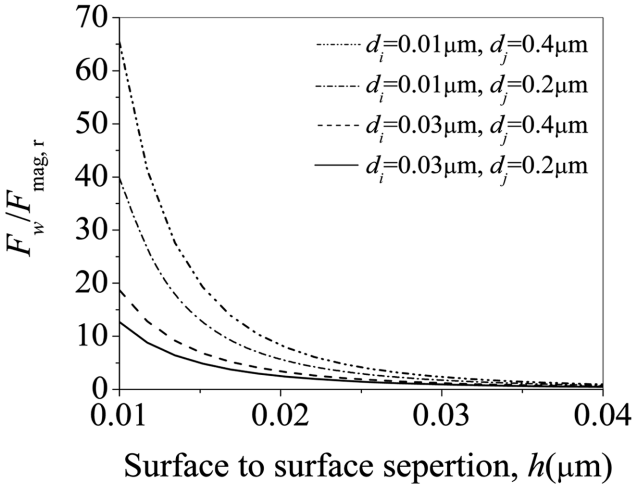

Fig. 4. Comparison of van der Waals force with magnetic dipole radial force.

with increase in the separation between the two particles. Although the van der Waals force is attractive and varies considerably with the size of the particles, it is short-ranged and can be neglected at separations larger than 0.03 μm.

1-5. Gravity

The particle gravity is given by

$$\mathbf{F}_g = \frac{\pi \rho_p d_p^3}{6}\mathbf{g} \tag{13}$$

Where **g** is the gravity acceleration.

2. Calculation Method

Two interacting magnetized particles move and approach each other in gas flow, under the action of several forces, such as magnetic dipole, drag, Brownian, van der Waals and gravity. Considering the relative motion between the two particles, particle i (nuclear particle) is set at the origin of the rectangle coordinates, and particle j (dust particle) approaches particle i (Fig. 5). The procedure for calculating the aggregation coefficient is as follows:

(1) Calculate all the trajectories in three-dimensional space in

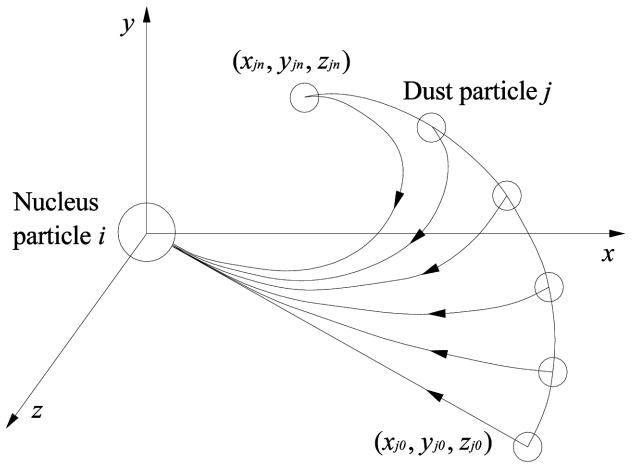

Fig. 5. Schematic diagram of relative trajectories of two interacting particles.

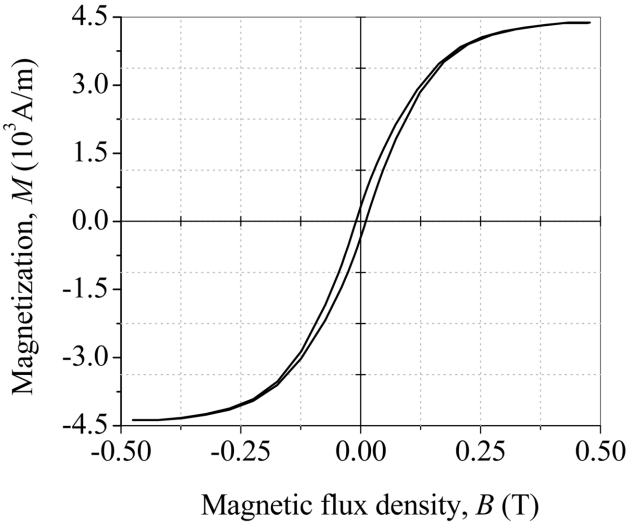

Fig. 6. Hysteresis loop of fly ash particles.

which dust particle j collides with nuclear particle i in unit time, and then determine all initial points of the trajectories, such as (x_{j0}, y_{j0}, z_{j0}) and (x_{jn}, y_{jn}, z_{jn}).

(2) All the initial points constitute a space, in which the two particles can collide in unit time, and the volume of the space is the value of aggregation coefficient between the two particles. So the aggregation coefficient can be acquired by calculating the volume of the space.

RESULTS AND DISCUSSIONS OF AGGREGATION COEFFICIENT

1. Calculation Conditions

The fly ash particles used in the binary collision-aggregation model were sampled from the hopper of the fourth electrical field of electrostatic precipitators (ESP) for tangential bituminous coal-fired utility boilers in Dalateqi power plants of China. The coal fired in

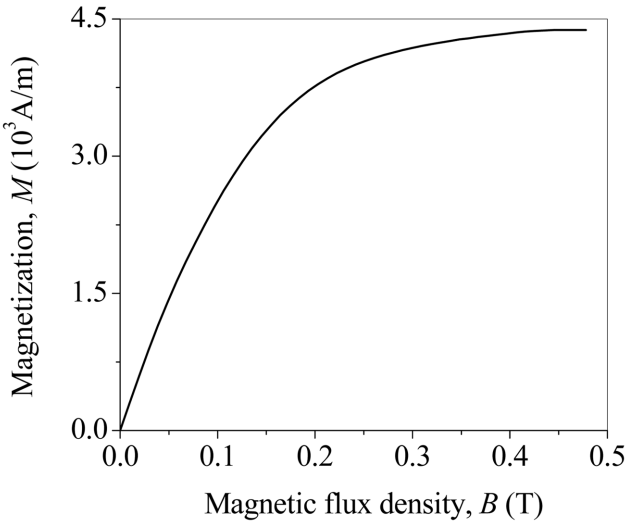

Fig. 7. Magnetization curve of fly ash particles.

Table 1. Physical parameters used in the binary collision-aggregation model

ρ_p (kg m^{-3})	μ (Pa s)	λ (m)	$u_{f,x}$ (m s^{-1})	$u_{f,y}$ (m s^{-1})	$u_{f,z}$ (m s^{-1})	T (K)
2200	1.83×10^{-5}	7.33×10^{-8}	0.08	0	0	293

the boiler is from Dongsheng, China. Fig. 6 and Fig. 7, respectively, show the hysteresis loop and magnetization curve of fly ash particles which were measured by Vibrating Sample Magnetometer (Lake Shore, 7400). With increase in the magnetic flux density, the particle magnetization rises rapidly in the beginning, and then attains its saturation value of 4.4×10^3 A m^{-1} at magnetic flux density (B) greater than 0.45 T. The magnetization of particles used in the model can be obtained from the magnetization curve (Fig. 7). All of the studies were carried out using nitrogen as gas medium at room temperature. Gas flows along x-axis; and gravity and magnetic flux density are aligned in the directions of y-axis and z-axis, respectively (Fig. 1). Other conditions in our studies are offered in Table 1.

RESULTS AND DISCUSSIONS

Particle-particle aggregation results from the their relative motion. In a uniform magnetic field, the fine fly ash particles approach each other under the combining action force of magnetic dipole, drag, Brownian, van der Waals and gravity. Particle size is a common factor in the magnitude of all those forces acting on individual particles, and magnetic flux density is another factor in the magnitude of magnetic dipole force, which is the most important applied force promoting particle aggregation. Thus, particle aggregation is primarily influenced by the particle size and the magnetic flux density.

Increasing the approach speed between interacting particles would promote aggregation and raise the aggregation coefficient. With an increase in the particle size, the magnetic dipole force rises so that particles approach each other more rapidly. Fig. 8 presents the effect of the sizes of the nuclear particles (d_n) and the dust particles (d_d) on the aggregation coefficient. Bigger sizes of particles results in higher values of aggregation coefficient, due to the magnetic dipole force being higher. Gravity difference between two particles is one

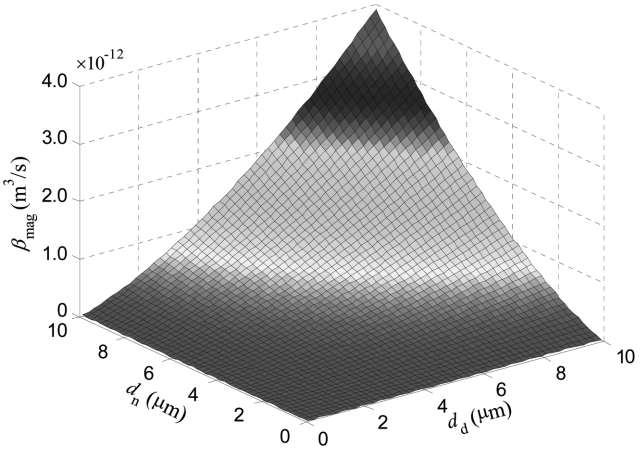

Fig. 8. Effect of particle size on aggregation coefficient regardless of gravity (B=0.47 T).

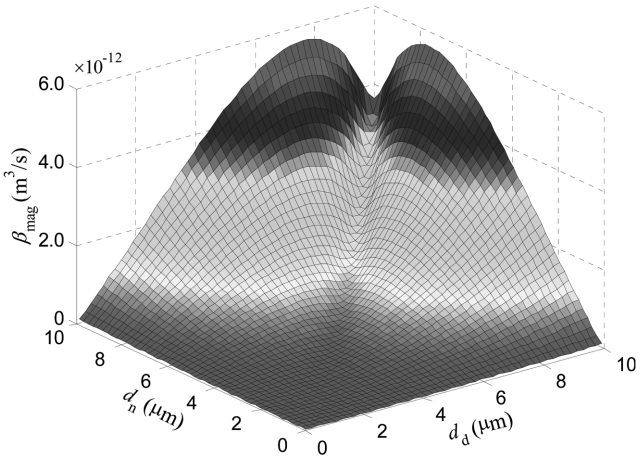

Fig. 9. Effect of particle size on aggregation coefficient considering gravity (B=0.47 T).

of the causes of their relative motion. The bigger the size difference between the two particles is, the more strongly gravity difference promotes aggregation. When the two particles' sizes are the same, the gravity difference is zero so that there is no effect of the gravity difference on particle aggregation. Fig. 9 gives the results above-mentioned.

The increase in the magnetic flux density enhances the magnetization of fly ash particles so that magnetic interaction force rises accordingly. Consequently, the aggregation coefficient increases with the magnetic flux density before particles are saturatedly magnetized, shown in Fig. 10. The aggregation coefficient increases significantly at magnetic flux density less than 0.25 T. At the magnetic flux density greater than that value, the aggregation coefficient increases slowly and reaches its maximum at 0.45 T.

PARTICLE REMOVAL EFFICIENCY

It was mentioned in the second section that the variation rate of particle number concentration can be calculated by solving the GDE when particle size distribution and aggregation coefficient are acquired. Fig. 11 gives the original size distribution of fly ash parti-

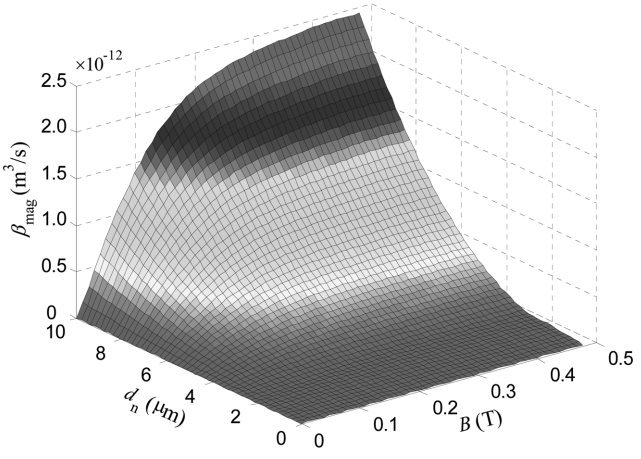

Fig. 10. Effect of magnetic flux density on aggregation coefficient (dust particle diameter is 2.5 μm).

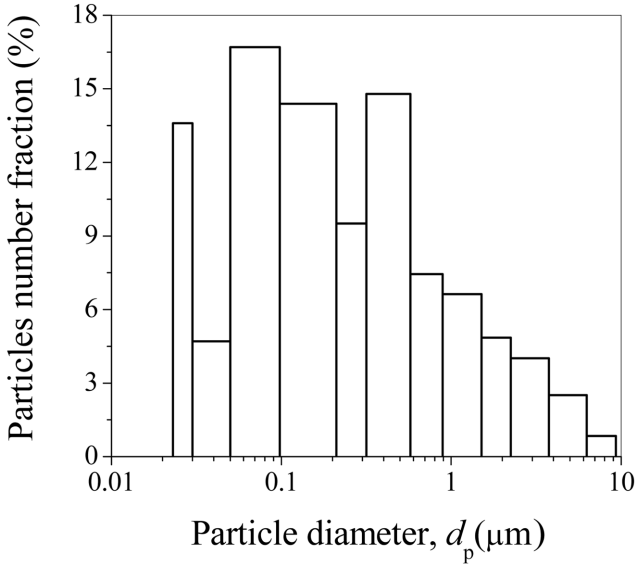

Fig. 11. Original size distribution of fly ash particles (d_{nmd}=0.151 μm).

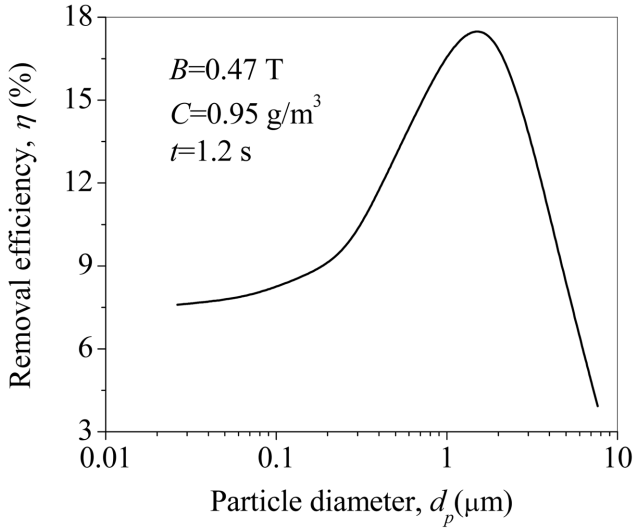

Fig. 12. Removal efficiency of different size particles (d_{nmd}=0.132 μm).

cles used in our studies whose number median diameter (d_{nm}, the particle diameter such that 50% of the particles by number are of smaller diameter) is 0.151 μm. The calculation method of the aggregation coefficient has been put forward above and analyzed in detail. Particle removal efficiency is a relative decrement in particle number concentration during a period of time. In this paper, section algorithm [26] is used to solve the GDE due to its simplicity and accuracy.

According to the section algorithm, in one section, the variation of particle number concentration results from the following four kinds of aggregations:

(1) A particle in this section aggregates with a smaller particle from any lower section. The resulting new particle remains in this section or is added to a higher section.

(2) Both particles in this section aggregate. The resulting new particle remains in this section or is added to a higher section.

(3) A Particle in this section aggregates with a bigger particle from any higher section. The resulting new particle is added to a higher section.

(4) Two smaller particles from lower sections aggregate. The resulting new particle is added to this section.

Therefore, if the aggregation coefficient and number concentration of the fly ash particles do not change with the particle size, the removal efficiencies of smaller particles are higher than the bigger ones. However, the aggregation coefficient and number concentration of particles greatly depend on their sizes (Fig. 9 and Fig. 11). Fig. 12 shows the removal efficiency when magnetic flux density (B), mass concentration (C) and particle residence time (t) in magnetic field are, respectively, 0.47 T, 0.95 g m^{-3} and 1.2 s. In the size range of 0.023-9.314 μm, the removal efficiencies of the mid-sized particles are higher than those of the smaller and the bigger ones. Particle aggregation also results in a change in particle size distribution which can be described by the number median diameter. In Fig. 12, as a result of aggregation, the particle number median diameter decreases from original 0.151 μm to final 0.132 μm. The decrease in number median diameter indicates that big particles can be more easily aggregated to larger particles than the smaller ones in the size range of 0.023-9.314 μm.

Total removal efficiency is a relative decrement in total particle number concentration in the size range of 0.023-9.314 μm. Aggregation coefficient, particle number concentration and particle residence time in a magnetic field are three main factors in aggregation. The increase in the aggregation coefficient and number concentration can bring on a higher collision frequency. So the total particle removal efficiency can be enhanced by raising the magnetic flux density and particle mass concentration (Fig. 13 and Fig. 14). At the same time, the particle number median diameter decreases accordingly. When particles are saturatedly magnetized, the aggrega-

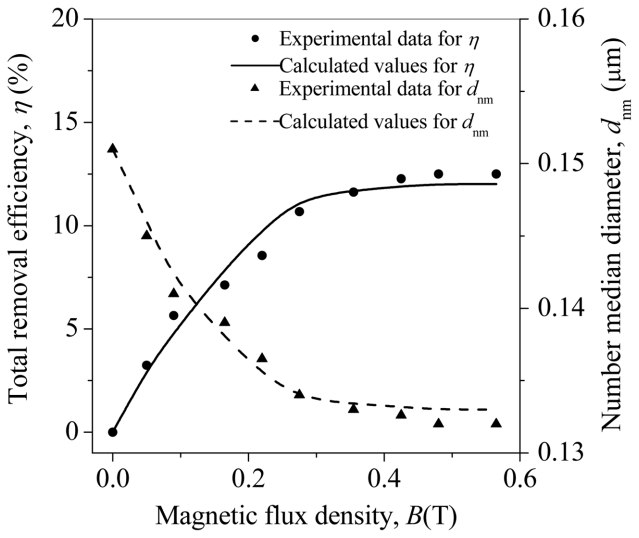

Fig. 13. Effect of magnetic flux density on total removal efficiency and number median diameter (C=0.95 g m^{-3}, t=1.2 s).

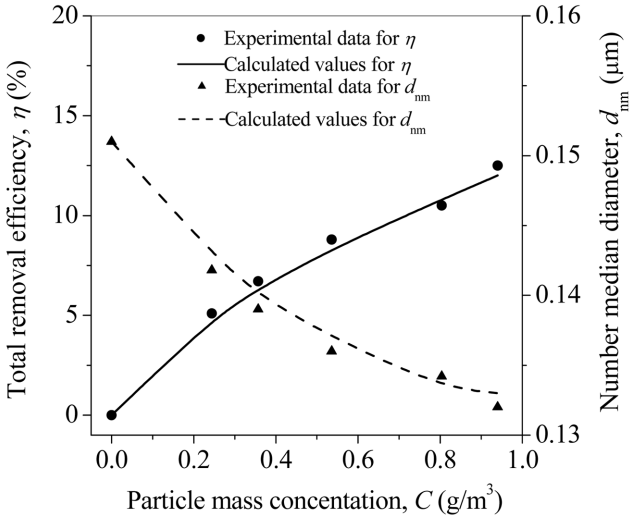

Fig. 14. Effect of particle mass concentration on total removal efficiency and number median diameter (B=0.45 T, t=1.2 s).

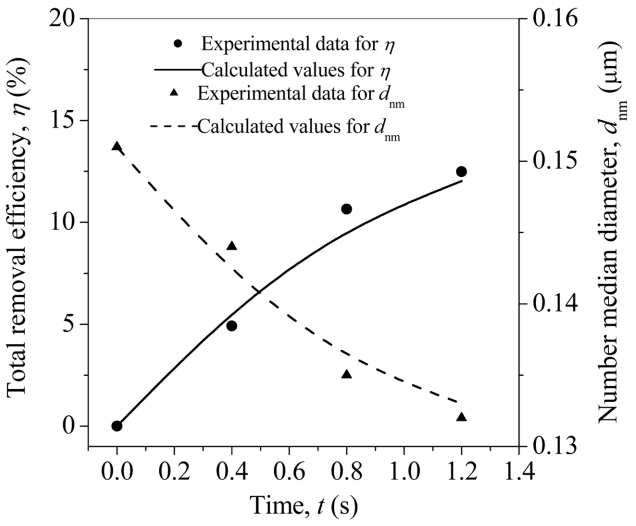

Fig. 15. Effect of aggregation time on total removal efficiency and number median diameter (B=0.45 T, C=0.95 g m^{-3}).

tion coefficient attains its maximum value (Fig. 8), so that the total removal efficiency also attains its maximum value (Fig. 12). Prolonging the particle residence time in the magnetic field, the total particle removal efficiency rises because of the increase in the interparticle collision times, as shown in Fig. 15. Moreover, Fig. 15 also illustrates that the particle number median diameter decreases with increase in the total removal efficiency. Moreover, the standard deviations between the calculated and the experimental values[1] of the total removal efficiency with the variations of magnetic flux density (Fig. 13), particle mass concentration (Fig. 14), and residence time (Fig. 15) are 7.2%, 8.1% and 9.6%, and those of particle number median diameter are 3.1%, 4.2% and 5.3%, respectively. So the two sets of results are essentially in agreement, indicating that the binary collision-aggregation model can be readily used.

[1]The experimental results have been reported in the paper "Experimental study on aggregation of inhalable particulate matter from coal combustion in uniform magnetic field". This paper was accepted by the journal of Proceedings of the CSEE.

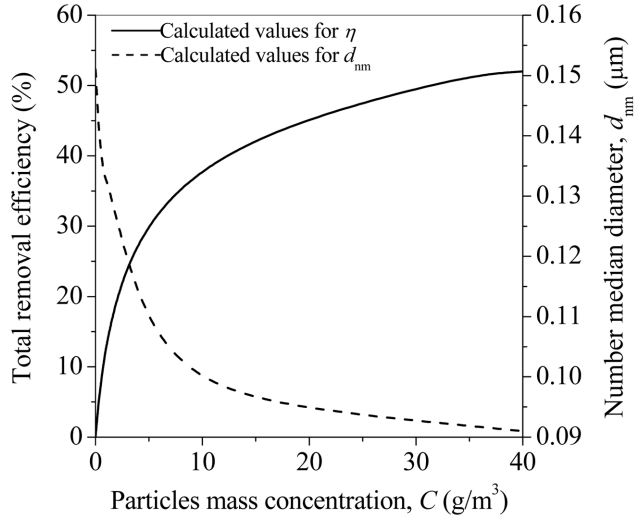

Fig. 16. Prediction of total removal rate of particle by numerical simulation (B=0.45 T, t=1.2 s).

In a practical dust removal system, the mass concentration of fly ash particles is far greater than that in the experiments. For the fly ash particles with higher mass concentration, the total removal efficiency and their number median diameter can be predicted by numerical simulation and the predicted results are shown in Fig. 16. The increase in the particle mass concentration causes a considerable increment in the total removal efficiency and decrement in the number median diameter. The total removal efficiency and number median diameter reach 52% and 0.091 μm at B=0.45 T, t=1.2 s and C=40 g m^{-3}.

It is very clear that particle aggregation is mainly affected by the aggregation coefficient, particle mass concentration and particle residence time in a magnetic field. Although the aggregation coefficient can attain its maximum value when particles are saturatedly magnetized, the saturation magnetization is lower than that of the magnetic particles. Thus, the aggregation coefficient can be effectively increased by magnetic seeding. Residence time is primarily limited by the geometrical size of the effective magnetic field. Therefore, magnetic seeding and magnetic field enlarging will be suggested promoting aggregation and increasing removal efficiency. Nevertheless, the decrease in the particle number median diameter is a disadvantageous factor in particle aggregation because the bigger particles are more easily aggregated than the smaller ones. That is, the higher the removal efficiency is, the more slowly the removal efficiency increases, which is demonstrated in Fig. 16.

CONCLUSIONS

Aggregation of fine fly ash particles in the size range of 0.023-9.314 μm transported by gas medium in uniform magnetic field was studied in this work. A binary collision-aggregation model was developed to investigate particle aggregation in a uniform magnetic field. Primary forces acting on particles, including magnetic dipole, drag, Brownian, van der Waals and gravity, were examined in the

model. The General Dynamic Equation (GDE) was then used to evaluate the particle removal efficiency and number median diameter. The calculated results were compared with the experimental data.

Model calculations show that the aggregation coefficient increases with the particle size and the magnetic flux density. The bigger the size difference between two particles is, the more strongly the gravity difference between them promotes aggregation. The removal efficiencies of the mid-sized particles are higher than those of the smaller ones and the bigger ones. The total removal efficiency can be enhanced by increasing magnetic flux density, particle mass concentration and particle residence time in the magnetic field. When particles are saturatedly magnetized, the total removal efficiency attains its maximum value, which is similar to its effect on the aggregation coefficient. As a result of aggregation, the particle number median diameter decreases with an increase in the total removal efficiency. A comparison between the model calculations and experimental data indicates that the two sets of results essentially agree. Therefore, the performance of the model is considered satisfactory. Nevertheless, the total particle removal efficiency is low because of the low aggregation coefficient and mass concentration and short particle residence time in a magnetic field. Thus, magnetic seeding and magnetic field enlarging were suggested, raising the total particle removal efficiency. And these are subjects of further research.

ACKNOWLEDGMENT

Financial support from the National Key Basic Research Program of China (No. 2002CB211600), Innovative Project for Graduate students in university of Jiangsu province and Excellent Ph. D. Thesis of Southeast University are sincerely acknowledged. The authors also express sincere gratitude to Drs. Anthony and Leckner for presenting us valuable advice.

NOMENCLATURE

A : Hamaker constant [J]
B : magnetic flux density [T]
C : mass concentration of particles [kg m^{-3}]
C_c : Cunningham correction factor
d_d : dust particle diameter [μm]
d_n : nuclear particle diameter [μm]
d_{nmd} : number median diameter [μm]
d_p : particle diameter [μm]
F_B : Brownian force [N]
F_d : drag force [N]
F_g : gravity force [N]
F_{mag} : magnetic dipole force [N]
F_W : van der Waals force [N]
g : gravity acceleration
G : Gaussian random number with zero-mean unit-variation
h : surface-to-surface separation between two particles [μm]
k : Boltzmann constant=1.38×10^{-23} [J K^{-1}]
m_o : magnetic moment of particle [A m^2]
M : magnetization of particle [A m^{-1}]
n : size distribution of particle [m^{-6}]
r : center-to-center distance of two interacting particles [m]
t : residence time of particle in magnetic field [s]
T : absolute temperature [K]
u_f : velocity of gas flow [m s^{-1}]
v_{min}, v_{max} : minimum and maximum volume of particles existing in gas flow [m^3]
v_p : velocity of particle [m s^{-1}]

Greek Letters

β_B : Brownian aggregation coefficient [m^3 s^{-1}]
β_{mag} : magnetic aggregation coefficient [m^3 s^{-1}]
Δt : magnitude of time step [s]
η : removal efficiency of particle [%]
θ : angle between magnetic moment vector and radial direction [rad]
λ : mean free path of gas molecules [m]
μ : dynamic viscosity [Pa s]
μ_0 : permeability of free space=$4\pi\times10^{-7}$ [N A^{-2}]
ρ_p : particle density [kg m^{-3}]
φ : magnetic scalar potential [J]
ψ : magnetic potential between two particles [J]

Subscripts

x, y, z : components along x-row, y-row and z-row directions
i, j : particles i and j
r, θ : components along radial and tangential direction

REFERENCES

1. C. Saskia and D. Z. Ven, *Atmospheric Environment*, **32**, 3717 (1998).
2. Y. W. Li, G L. Yang, F. G Li and L. S. Yu, *Opto-Electronic Engineering*, **32**, 54 (2005).
3. Y. L. Jin, G L. He, F. Liu, Y. F. Hong, Y. B. Cheng, H. Z. Wang, B. X. Zhao, X. W. Deng, L. Liu and Y. P. Zhang, *Journal of Hygiene Research*, **31**, 342 (2002).
4. X. Guo, C. G Zheng and T. Sun, *Journal of Combustion Science and Technology*, **11**, 192 (2005).
5. J. M. Sun, *Acta Mineralogical Sinica*, **21**, 14 (2001).
6. Y. C. Zhao, J. Y. Zhang, Q. Gao, X. Guo and C. G Zheng, *Proceedings of the CSEE*, **26**, 82 (2006).
7. M. R. Parker, R. P. A. R. Van Kleef, H. W. Myron and P. Wyder, *Journal of Colloid and Interface Science*, **101**, 314 (1984).
8. L. Petrakis, P. F. Ahner and F. E. Kiviat, *Separation Science and Technology*, **16**, 745 (1981).
9. J. Svoboda and T. Fujita, *Minerals Engineering*, **16**, 785 (2003).
10. T. Zarutskaya and M. Shapiro, *Journal of Aerosol Science*, **31**, 907 (2000).
11. H. Nübold, T. Poppe, M. Rost, C. Dominik and K. H. Glassmeier, *Icarus*, **165**, 195 (2003).
12. A. T. Zimmer, Ph.D. thesis, AAQRL, University of Cincinnati, Cincinnati, OH (2000).
13. T. Y. Ying, S. Yiacoumi and C. Tsouris, *Chemical Engineering Science*, **55**, 1101 (2000).
14. Z. G Forbes, B. B. Yellen, K. A. Barbee and G Friedman, *IEEE Transactions on Magnetics*, **39**, 3372 (2003).
15. S. Yiacoumi, D. A. Rountree and C. Tsouris, *Journal of Colloid and Interface Science*, **184**, 477 (1996).

16. J. Svoboda, *IEEE Transactions on Magnetics*, **18**, 796 (1982).
17. C. Dominik and H. Nübold, *Icarus*, **157**, 173 (2002).
18. K. Prakash and B. Pratim, *Journal of Aerosol Science*, **36**, 455 (2005).
19. J. P. Kim, I. S. Han and C. B. Chung, *Korean J. Chem. Eng.*, **20**, 580 (2003).
20. C. G. Moniruzzarnan and K. Y. Park, *Korean J. Chem. Eng.*, **23**, 159 (2006).
21. M. Smoluchowski, *Zeitschrift für Physikalische Chemie*, **92**, 129 (1917).
22. Y. Koizumi, M. Kawamura, F. Tochikubo and T. Watanabe, *Journal of Electrostatics*, **48**, 93 (2000).
23. Y. Nakajima and S. Takashi, *Powder Technology*, **135-136**, 266 (2003).
24. K. Fukagata, S. Zahrai and F. H. Bark, *Heat and Mass Transfer*, **40**, 715 (2004).
25. A. D. Ebner, J. A. Ritte and H. J. Ploehn, *Journal of Colloid and Interface Science*, **225**, 39 (2000).
26. D. J. Kim and K. S. Kim, *Korean J. Chem. Eng.*, **19**, 495 (2002).